

On the Pitfalls of Batch Normalization for End-to-End Video Learning: A Study on Surgical Workflow Analysis

Dominik Rivoir^{1,2}, Isabel Funke^{1,2}, Stefanie Speidel^{1,2}

¹Translational Surgical Oncology, National Center for Tumor Diseases (NCT) Dresden, Germany,

²Centre for Tactile Internet (CeTI), TU Dresden, Germany

{dominik.rivoir, isabel.funke, stefanie.speidel}@nct-dresden.de

Abstract

Batch Normalization's (BN) unique property of depending on other samples in a batch is known to cause problems in several tasks, including sequential modeling. Yet, BN-related issues are hardly studied for long video understanding, despite the ubiquitous use of BN in CNNs for feature extraction. Especially in surgical workflow analysis, where the lack of pretrained feature extractors has led to complex, multi-stage training pipelines, limited awareness of BN issues may have hidden the benefits of training CNNs and temporal models end to end. In this paper, we analyze known as well as novel pitfalls of BN in video learning, including issues specific to online tasks such as a 'cheating' effect in anticipation. We observe that BN's properties create major obstacles for end-to-end learning. However, using BN-free backbones, even simple CNN-LSTMs beat state of the art in two surgical tasks by utilizing adequate end-to-end training strategies which maximize temporal context. We conclude that awareness of BN's pitfalls is crucial for effective end-to-end learning in surgical tasks. By reproducing results on natural-video datasets, we hope our insights will benefit other areas of video learning as well. Code: https://gitlab.com/nct_tso_public/pitfalls_bn.

1. Introduction

Batch Normalization (BatchNorm/BN) [31] is a highly effective regularizer in visual recognition tasks and is ubiquitous in modern Convolutional Neural Networks (CNNs) [25, 60, 61]. It is, however, also considered a source for silent performance drops and bugs due to its unique property of depending on other samples in the batch and the assumptions tied to this [9, 67, 68]. Most notably, BatchNorm assumes that batches are a good approximation of the training data and only performs well when batches are large enough and sampled i.i.d. [31, 68].

This generally does not hold for sequence learning, where batches contain highly correlated, sequential samples, and has led to the use of alternatives such as Layer-Norm (LN) [4] in NLP [53, 65]. In video learning, BN has been studied less [10, 67] especially in long-video tasks.

In long-video tasks (e.g. action segmentation), CNNs are only used to extract image- or clip-wise features using pretrained CNNs (e.g. [11]) off-the-shelf. Only the temporal model, which typically does not use BN, is trained to aggregate features over time [1, 18, 29, 32, 37, 52, 66, 76]. However, in specialized small-data domains such as surgical video, well-pretrained CNNs may not be available [14, 79], requiring CNNs to be finetuned, either through 2-stage [12] or end-to-end (E2E) training [33]. The latter seems preferable to enable joint learning of visual and temporal features, especially since spatio-temporal feature extractors (e.g. 3D CNNs) have not been effective on small-scale surgical datasets [14, 79]. However, BN layers in CNNs pose obstacles for end-to-end learning.

We hypothesize that BN's problems with correlated, sequential samples have silently caused research in video-based surgical workflow analysis (SWA) to head into a sub-optimal direction. The focus has shifted towards developing sophisticated temporal models to operate on extracted image features similar to the natural-video domain, replacing end-to-end learning with complex multi-stage training procedures, where each component (CNN, LSTM [27], TCN [18], Attention [65], etc.) is trained individually [5, 22, 36, 46, 77]. We argue that even simple CNN-LSTM models can outperform these methods when BN-free backbones are used and the model is trained end to end.

We investigate BatchNorm's pitfalls in end-to-end learning on two SWA tasks: *surgical phase recognition* [62] and *instrument anticipation* [50]. We choose these for two reasons: The lack of well-pretrained feature extractors and ineffectiveness of 3D CNNs signify the need for end-to-end approaches in SWA and thus make BN-issues most relevant here. Further, SWA is one of the most active research areas for *online* video understanding, where models are con-

strained to access only past frames, causing additional BN problems regarding leakage of future information.

Our contributions can be summarized as follows: We (i) challenge the predominance of multi-stage approaches in surgical workflow analysis (SWA) and show that awareness of BN’s pitfalls is crucial for effective end-to-end learning, (ii) provide a detailed literature review showing BN’s impact in SWA, (iii) and analyze when BN issues occur, including problems specific to online tasks such as “cheating” in anticipation. Further, we (iv) show that the common solution *FrozenBN* is not always effective, (v) beat state-of-the-art in two SWA tasks with simple end-to-end approaches by avoiding BN entirely and (vi) reproduce our main findings on other datasets from the natural-video domain.

2. Background & Related Work

2.1. Batch Normalization and Beyond

BatchNorm [31] is used in almost all modern CNNs. It is assumed to have a regularizing effect, improve convergence speed and enable training of deeper networks [6, 15, 28]. In BatchNorm, features x are standardized by estimating the channel-wise mean and variance and then transformed using an affine function with learnable parameters γ, β . Formally, $BN(x) = \gamma \frac{x - E(x)}{\sqrt{Var(x) + \epsilon}} + \beta$, where $E(x)$ and $Var(x)$ are the mean and variance estimates calculated from the current batch during training. During inference, when the concept of batches is generally not applicable anymore, a running average of the training values of $E(x)$ and $Var(x)$ is used to estimate the global dataset statistics.

Despite BN’s popularity and success, it has major disadvantages. The discrepancy between train and test behavior can lead to drops in performance when batch statistics are poor estimates of global statistics, e.g. when batches are small or contain correlated samples. Also, BN’s property of depending on other samples in the batch can lead to hidden mistakes if not handled with care. Resulting problems have been observed in many areas such as object detection [67, 68], sequence modeling [4], reinforcement learning [51], continual learning [48], federated learning [3] and contrastive learning [26]. E.g. in language modeling, both aforementioned issues are highly problematic and have lead to the use of alternative normalization layers [4, 53, 65].

CBN [73], EvalNorm [57] and others [30, 70, 71] are extensions of BN which address some of these issues. Normalization layers which only operate on single samples (e.g. GroupNorm [67], LayerNorm [4]) have also been proposed [4, 39, 41, 56, 64, 67]. DNR [10] proposed recurrent estimation of affine parameters for video models but does not address the discrepancy of batch and global statistics.

Wu et al. [68] provide the most extensive review of BN issues for vision to date, including train-test discrepancies, the effect of batch sizes and correlated samples as well as

Table 1. Previous approaches for video-based surgical workflow tasks. End-to-end approaches on short sequences have been proposed initially. Recent research has favored multi-stage approaches where each model component is trained separately.

(✓) = contains an end-to-end stage)

Methods	BN	End2End	Train stages	Remarks
AL-DBN[7], Rivoir et al.[50]	✗	✓	1	End-to-end CNN-LSTM ✗ <i>non-SOTA backbone (AlexNet)</i>
SV-RCNet[16], MTRCNet[34]	✓	(✓)	2	CNN-LSTM w/ end-to-end stage ✗ <i>many short sequences per batch</i>
TMRNet[35], LRTD[54]	✓	(✓)	2	SV-RCNet + Attention ✗ <i>many short sequences per batch</i>
CataNet[46]	✓	(✓)	4	CNN-LSTM w/ end-to-end stage ✗ <i>requires 4 training stages</i>
TransSVNet[22], TeCNO[12] and [2, 13, 47, 75, 77, 79, 81]	✓	✗	2-3	CNN+(RNN,TCN,Transformer) ✗ <i>separate training stages for each model component</i>
Proposed	✗	✓	1	End-to-end CNN-LSTM <i>SOTA using BN-free backbones</i>

solutions such as FrozenBN [68] or redefining over which samples to normalize. Related to our work, they show problems of small batches for estimating batch statistics and discuss cheating behavior in object detection and contrastive learning. Consequences for video are only hypothesized. In another work [67], Wu et al. show how BN hides the benefit of higher frame rates for clip-based action classification.

Recently, there has been a trend towards CNNs without BN. Brock et al. [9] discuss disadvantages of BN and propose a class of normalizer-free networks *NFNet*. They, however, require custom optimizers and are sensitive to hyperparameters. Finally, *ConvNeXt* [43] is a CNN competitive with Vision Transformers [16]. It replaces BatchNorm with LayerNorm although this was not the focus of the paper.

2.2. Online Surgical Workflow Analysis

Surgical Workflow Analysis (SWA) [45] is a broad set of tasks which aim at understanding events and their interrelations in recorded or live surgical videos. SWA covers a wide range of common computer vision problems including temporal segmentation (e.g. surgical phase recognition [62]), dense frame-wise regression (e.g. anticipating instrument usage [50] or procedure duration [63]) or video classification (e.g. early surgery type recognition [36]). SWA tasks are inherently video-based as they require understanding the sequence of events which have occurred until the current time point and often require memorizing long-range dependencies. The overall goal is to provide live, context-aware assistance during surgery [44]. Thus, tasks are mostly defined as online recognition problems [12, 36, 50, 63].

Most approaches to surgical workflow tasks combine a 2D CNN for frame-wise feature extraction with a temporal model (e.g. LSTM, TCN or Attention) for aggregation over time. In the following, we discuss different learning strategies which have emerged for surgical workflow tasks and how they were possibly influenced by BN-related problems. Table 1 provides an overview of our findings.

E2E without BN: Early methods completely avoid BN-issues by using backbones without BatchNorm. End-to-end

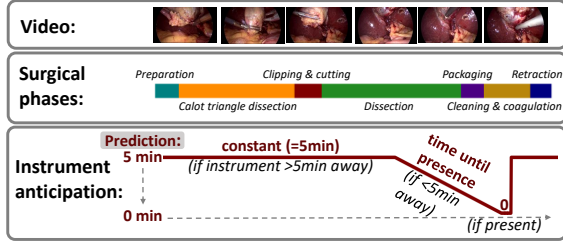


Figure 1. Two online surgical workflow tasks: *phase recognition* and *instrument anticipation* on the Cholec80 dataset [62]

CNN-LSTM models with AlexNet [38] or VGG [55] backbones have been proposed for phase recognition [7, 74], anticipation [50], duration prediction [49, 74], surgery type prediction [36] and occlusion detection [5]. All methods train long sequences of several minutes. However, results are not competitive due to the use of outdated backbones.

E2E with BN: SV-RCNet [33] and MTRCNet [34] are two examples of end-to-end ResNet-LSTM models for phase recognition. However, to minimize the discrepancy between batch and global statistics, training sequences are only 10 frames long (2 and 10 seconds, respectively) and processed in large batches of 100 sequences. TMRNet [35] and LRTD [54] extend SV-RCNet with attention blocks to learn long-range dependencies. Still however, sequences of only 10 frames are trained end to end. CataNet [46] proposes a complex, 4-stage learning process for ResNet-LSTMs to predict surgery duration. In one of the stages, end-to-end learning on long sequences is made possible by using FrozenBN with global statistics from a previous stage.

Multi-stage: Recently, methods have shifted towards more complex temporal models with pretrained visual features, circumventing BN-issues. A CNN is first trained on randomly sampled image batches, followed by a temporal model trained on extracted image features. Methods in this style have been proposed for phase recognition [12, 13, 22, 75, 81], duration prediction [2, 8, 63], tracking [47] or anticipation [77]. Most notably, TeCNO [12], an MS-TCN [18] trained on ResNet features, is the popular approach for 2-stage learning and Trans-SVNet [22], a 3-stage method which trains a Transformer on TeCNO features, is among the state of the art in phase recognition.

Awareness for BN issues: Although BatchNorm has possibly influenced the move towards complex, multi-stage or short-range models, its issues have rarely been discussed. Yengera et al. [74] selected AlexNet for efficiency reasons. Kannan et al. [36] simply state that VGG outperformed ResNet, but not whether this may be due to BatchNorm. The authors of SV-RCNet [33] do not explain their choice of short sequences despite large batch sizes. Nwoye et al. [47] justify their 2-stage approach through “fair comparison”. CataNet [46] uses FrozenBN (code), but it is not mentioned in the paper. Rivoir et al. [50] briefly mention cheating to

justify the choice for an AlexNet in instrument anticipation.

3D backbones: It is noticeable that surgical workflow methods almost unanimously use 2D CNNs as feature extractors. The specialized surgical domain requires backbones to be finetuned and several studies suggest that the small-scale public datasets available in this domain are not sufficient to train large 3D CNNs [14, 79]. Only few works achieve good results on larger private datasets [14, 78].

2.3. Action Segmentation & Anticipation

In the natural-video domain, action segmentation and anticipation can be viewed as workflow analysis tasks as they aim at understanding the composition of complex activities.

Training strategies: Methods avoid BatchNorm during temporal learning by almost exclusively relying on pretrained visual features [11] in both action segmentation [18, 29, 32, 66, 76] and anticipation [1, 20, 21, 37, 52]. Whether this development can be attributed to computational costs, the availability of well-pretrained feature extractors or BatchNorm’s properties is not yet clear.

Sener et al. [52] indicate limitations of pretrained visual features for action anticipation by showing a large performance gap compared to using ground-truth observed actions as input. The only end-to-end anticipation model for natural video of which we are aware (AVT [24]) does not use BatchNorm as it is entirely Transformer-based. Although not mentioned as motivation for this model choice, BN would likely have caused both train-test discrepancy and “cheating” since single-sequence batches are used. Recently, Liu et al. [42] show the effectiveness of end-to-end strategies for the related temporal action detection task. They use FrozenBN but do not discuss BatchNorm issues.

Online recognition: Online action understanding has mostly focused on temporal action detection [17, 40, 69, 80] or anticipation. Apart from few exceptions [23], action segmentation is usually done offline [18, 29, 32, 66, 76].

3. Making End-to-End Video Learning Work

We analyze limitations and impact of BatchNorm for end-to-end learning on two surgical tasks (Fig. 1). In *surgical phase recognition*, an online temporal segmentation task, we show how BatchNorm can affect training strategies and performance. Then, we demonstrate BatchNorm’s ability to access future frames in online tasks through a “cheating” phenomenon in *surgical instrument anticipation*.

3.1. Proposed End-to-End Learning Strategies

Our premise is that end-to-end learning is preferable over multi-stage approaches and thus we propose a simple, intuitive strategy for training CNN-LSTM models on online surgical workflow tasks. We use the LSTM to demonstrate that even simple temporal aggregation can

be effective when visual features are improved through end-to-end learning. We also argue that recurrent, state-based models, where a memory state propagates information through time, are often well suited for online recognition tasks [20, 21, 23]. Especially for end-to-end learning on partial video sequences, the LSTM’s hidden state can be utilized to larger temporal context. We propose:

End-to-end training: Optimize the feature backbone and temporal model end-to-end in a single training stage.

Sequential batches: Use fully-sequential batches (i.e. one sequence per batch) to maximize the length of training sequences for the given memory constraints.

Carry-hidden training (CHT) (optional): Select batches in temporal order. This way, the LSTM’s detached hidden state can be carried across batches to provide more temporal context during training.

Partial freezing (optional): Freeze bottom layers of the backbone to increase the length of training sequences. Although this is not fully end to end anymore, the main benefits are still given: There is still only a single training stage and image features are optimized in a temporal context.

3.2. BatchNorm Problems with Sequential Batches

In previous work, the proposed strategy is not used due to incompatibility with BatchNorm. The main problems are:

1) Train-test discrepancy/small-batch effect: It is well-known that BatchNorm performs poorly with small batches [67, 68]. Training batch statistics only poorly estimate global statistics used during inference and thus induce a discrepancy between train and test behavior. However, when batches contain sequential video frames, even large batches lead to similar issues as the highly correlated samples also do not approximate global statistics well. Similar observations have been made in different contexts [4, 67].

2) Cheating/leakage: Previous work has discussed BatchNorm’s ability to leak information from other samples in the batch and its impact on performance in object detection or contrastive learning [68]. In online video tasks, a similar phenomenon can be fatal. BatchNorm can leak information from future frames, which allows models to “cheat” certain objectives and prevents learning useful features. This “cheating” phenomenon is most obvious in anticipation tasks. In *instrument anticipation*, the occurrence of an instrument influences the batch statistics of channels reacting to its appearance. During training, BN models may pick up on these fluctuations in batch statistics even at *earlier time points* within the same batch and use them anticipate the instrument’s later occurrence. Thus, the model only has to learn to *recognize* the instrument to solve the *anticipation* objective during training, but will fail during inference when batch statistics are not available.

3.3. Alternative Backbones without BatchNorm

We enable fully-sequential, end-to-end learning by replacing ResNet50 with existing BN-free CNNs. We use a ResNet50 with **GroupNorm (GN)** [67] for fair comparison as well as the more recent **ConvNeXt-T** [43], which uses ViT-style LayerNorm [72] and is of comparable size to ResNet50. We also investigate **FrozenBN** [42, 68], where batch statistics are replaced by global statistics from pre-training. All models are pretrained on ImageNet-1k [38].

3.4. Training Strategies in Previous Work

Pretrained feature extractors: In natural-video tasks such as action segmentation, pretrained 3D CNNs enable visual feature extraction with (short-range) temporal context. In the surgical domain, however, finetuning is required.

Multi-stage: Most surgical workflow methods resort to multi-stage training [2, 13, 12, 22, 47, 75, 77, 79, 81], where 2D backbones are trained on randomly sampled image batches, avoiding BN issues. This has several disadvantages. Firstly, it increases the number of hyperparameters since learning rate, number of epochs etc. have to be tuned for each training stage. Secondly, when backbone and temporal model are trained on the same data, overfitting on the image task can prevent the temporal model from learning useful features. For example, we found early stopping of the ResNet pretraining crucial to reproduce TeCNO’s [12] results. Yi et al. [75], who specifically promote multi-stage pipelines, require complex augmentation methods to prevent overfitting between stages. Lastly and most importantly, pretraining on single frames changes the dynamics of the task and cannot guarantee features that are suitable for the target task. A certain visual feature might only be relevant to the task in combination with a previous event. If the backbone does not learn to capture this feature during pretraining, this information is lost and cannot be recovered in the subsequent temporal-modeling stage.

End-to-end with multiple sequences: In end-to-end models, BatchNorm’s requirement of diverse batches can be fulfilled by including several, randomly drawn sequences in one batch (e.g. SV-RCNet [33]). However, this comes at the cost of shortening the individual training sequences in order to adhere to the overall memory limits. It also restricts possible training strategies like carrying hidden states of LSTMs across batches and can thus impair performance.

End-to-end with FrozenBN: FrozenBN is a popular ad-hoc solution in areas where BN causes problems, including end-to-end video learning [42, 46]. However, it removes the potential optimization benefits of normalization layers [68].

We compare our strategy to multi-stage as well as end-to-end training with multiple sequences and FrozenBN.

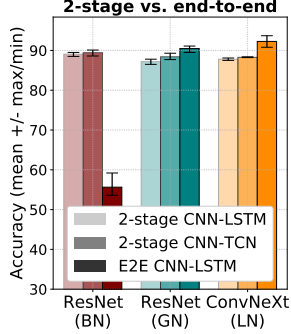
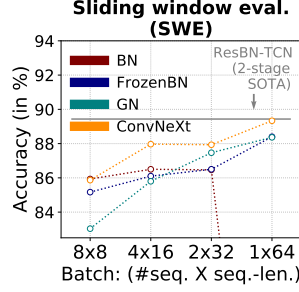
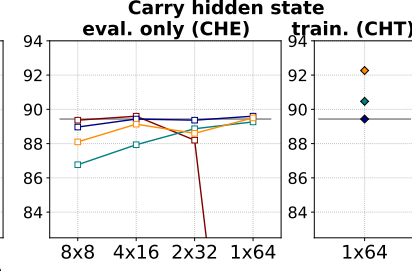


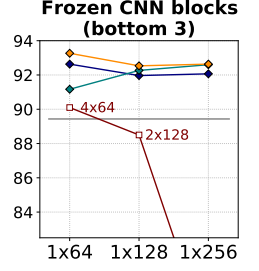
Figure 2. *Phase Recognition*: BN-free, end-to-end CNN-LSTMs outperform 2-stage LSTMs and TCNs. The widely-used ResNet50 with BN fails. Split: 40/8/32 from TeCNO [12].



(a) Length vs diversity



(b) CHT strategy improves BN-free models



(c) Partial freezing

Figure 3. *Phase Recognition*: (a) While longer sequences improve BN-free models, BN in ResNet50 backbones requires careful selection of the number of sequences per batch before performance drops. (b) Carrying hidden state through entire videos at test time improves models. By also doing this during training, train-test discrepancy is removed and models improve further. In BN models, implementing this is not straightforward. (c) BN models improve by freezing backbone blocks and thus increasing training sequences while maintaining batch diversity. Yet, freezing also improves BN-free models.

4. Experiments

We provide a comprehensive and detailed analysis of how BatchNorm affects end-to-end surgical workflow analysis. We show the advantage of end-to-end over 2-stage learning (*Hypothesis 1*), longer training sequences (*H.2*) and carrying hidden states across batches in online tasks (*H.3*) and how this can fail using BN-based backbones. We confirm our findings on similar, natural-video datasets (*H.4*) and other BN variants (*H.5*). Then, we discuss how freezing layers can alleviate BN-issues (*H.6*) and position our proposed models within the state of the art for surgical phase recognition (*H.7*). We show BN’s potential to cheat (*H.8*), provide evidence in instrument anticipation (*H.9*) and compare models to previous anticipation approaches (*H.10*).

4.1. Data, Tasks & Implementation Details

For all surgical tasks, we use the widely-studied *Cholec80 dataset* [62], which consists of 80 recorded gall-bladder removals (cholecystectomies). Videos range from 12 to 100 min (mean ca. 38 min), processed at 1fps with frame-wise labels for 7 instruments and 7 surgical phases.

Surgical phase recognition is an online dense temporal segmentation task [62]. We use the mean video-wise accuracy for evaluation (F1 in the appendix). To reproduce our claims on natural videos, we train the same models on online action segmentation on *GTEA* [19] and *50Salads* [59].

Instrument anticipation is an online frame-wise regression task. At each time point, the objective is to predict the remaining time until occurrence of an instrument within a horizon of 5 minutes. Outside the horizon, a constant should be predicted (see Fig. 1). We follow the recently proposed task formulation [50]. We use the weighted MAE (wMAE) as evaluation metric, where errors inside and outside the horizon are weighted equally to counteract imbalances.

For both tasks, we use 40 videos for training, 8 for vali-

dation and 32 for testing, following TeCNO [12]. Only for SOTA comparison in phase recognition, we retrain models on a 32/8/40 split from Trans-SVNet [22]. Epochs with the best validation score (*acc./wMAE*) are selected for testing. Runs are repeated 3 times. More details in the appendix.

4.2. Surgical Phase Recognition

Hypothesis 1: End-to-end outperforms 2-stage training, but not with BatchNorm. We argue that end-to-end learning is preferable over 2-stage approaches but fails when the backbone contains BatchNorm. To demonstrate this, we train CNN-LSTM models with three different backbones (Resnet50-BN, ResNet50-GN and ConvNeXt-T), sequential batches of 64 frames (1×64) and the proposed carry-hidden training (CHT). For comparison, we train each backbone in a 2-stage process with an LSTM or causal MS-TCN, following TeCNO’s training procedure [12].

Fig. 2 shows that end-to-end models outperform 2-stage approaches when using a backbone without BN. Only the typically used BN-based ResNet50 fails completely. While BatchNorm is known to fail with small batch sizes [67, 68], even large batch sizes lead to similar issues here due to the strong correlation of subsequent frames. In other words, a batch with a single 64-frame sequence behaves similar to a batch size of 1. The next paragraph presents more evidence.

Hypothesis 2: BatchNorm causes trade-off between sequence length and batch diversity. We investigate the effect of different batch configurations and follow SV-RCNet’s [33] strategy for end-to-end CNN-LSTMs: Multiple shorter sequences are sampled per batch, hidden states are reset after each training sequence and the LSTM uses a sliding window for evaluation (*SWE*) to ensure consistent sequence lengths at train and test time. We test this strategy using 1-8 sequences in batches of 64 frames in total.

In Fig. 3a, we observe that the performance of all BN-

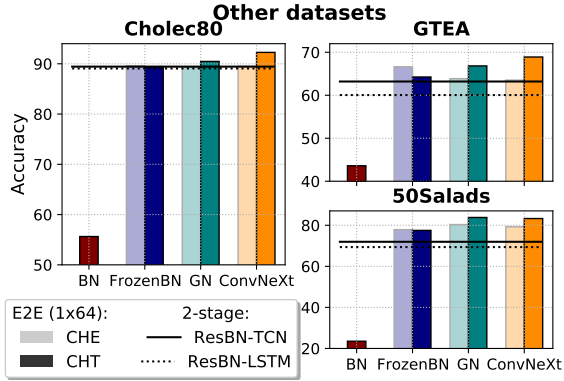


Figure 4. *Online action segmentation*: Results on surgical data (left) can be reproduced on natural-video datasets (right).

free models improves with fewer but longer sequences per batch since it increases the temporal context. In BN models, however, fewer sequences lead to a poor approximation of global statistics and we observe drops in performance despite the constant total batch size, similar to the frame-rate trade-off in video-clip classification [67]. The BN backbone outperforms its FrozenBN and GroupNorm counterparts for short sequences but stagnates and then collapses with longer ones. Due to this trade-off between sequence length and batch diversity, BN models eventually cannot reach the performance of the fully-sequential, BN-free models.

Hypothesis 3: BatchNorm restricts LSTM usage for online tasks. Note that by adopting SV-RCNet’s hidden-state handling, none of the methods outperform the 2-stage SOTA [12]. This is likely due to the short temporal context seen by the LSTM. Simply carrying the hidden state across the entire video during inference (*CHE*) already provides a clear performance boost without changing the training strategy (Fig. 3, *SWE* vs. *CHE*). Yet, this induces another train-test discrepancy since the LSTM accumulates hidden states over much longer time periods at test time compared to training time, which could cause unpredictable behavior.

In online tasks, however, the discrepancy can naturally be resolved by exploiting the fact that hidden states only flow in a single direction. Specifically, we can implement the proposed *carry-hidden training* (*CHT*) by selecting batches in temporal order and carrying the detached hidden states across batches during training as well.

With this approach, GN and ConvNeXt backbones outperform 2-stage and other end-to-end strategies (Fig. 3b). In BN models, however, this learning strategy is not implementable in a straightforward way since it requires selecting batches in temporal order, which violates the i.i.d. requirement. Thus, the train-test discrepancy in LSTMs remains.

Interestingly, the *CHT* strategy is not effective with FrozenBN. We found models often to collapse and finally only achieve subpar performance by lowering the initial learning rate. The lack of proper normalization with

Table 2. *Phase recognition*: BN alternatives for video (DNR [10]) or small batches (CBN [73]).

Accuracy (mean \pm std. over runs) on 40/8/32 split from TeCNO [12].			
End-to-end ResNet-LSTM w/ ...	4 \times 16, CHE	1 \times 64, CHE	1 \times 64, CHT
GN	87.9(\pm 0.8)	89.3(\pm 0.4)	90.5(\pm 0.9)
BN	89.6(\pm 1.0)	59.7(\pm 3.8)	55.6(\pm 3.1)
DNR [10] w/o Kinetics-400 pretraining	79.6(\pm 1.3)	54.2(\pm 3.9)	48.4(\pm 4.9)
CBN [73] w/ window size 1 (equiv. to BN, sanity check)	89.5(\pm 0.7)		
CBN [73] w/ burnin 3 epochs, window size 8 (original)	49.1(\pm 2.4)		
CBN [73] w/ burnin 10 epochs, window size 4	87.4(\pm 0.8)	79.4(\pm 1.3)	51.5(\pm 19.8)

FrozenBN might cause more instability than in GN or ConvNeXt models and we suspect that the non-i.i.d. selection of batches during *CHT* can encourage this. We present more evidence in our experiments on other datasets (Fig. 4) and a more detailed exploration of learning rates in the appendix.

Hypothesis 4: BatchNorm induces similar issues on natural-video datasets. Fig. 4 confirms our findings on small-scale datasets from the natural-video domain (*GTEA* and *50Salads*) by retraining the same models used for phase recognition on online action segmentation. We find that our main claims can be reproduced, namely that (1) BN-based end-to-end models fail, (2) end-to-end approaches without BN outperform 2-stage models and (3) the *CHT* strategy is effective using GN or ConvNeXt but not with FrozenBN.

Hypothesis 5: Other BatchNorm variants are not suitable. In Fig. 2, we compare to recent variants of BN: DNR [10] and CBN [73]. DNR proposes temporally dependent estimation of BN’s affine parameters to adjust to properties of batches in video settings. Yet, batch stats are still computed like in standard BN, so the train/test discrepancy with fully sequential batches remains. Due to unavailability, we do not use a pretrained DNR model, but model collapse with 1x64 batches can still clearly be seen. CBN reduces batch dependence by accumulating stats from multiple batches. Yet, for our proposed *CHT* strategy, CBN is not suitable due to strong inter-batch correlations of subsequent batches. Further, we found the transition to accumulated stats after its burnin phase to cause instability even in *CHE* settings, despite finetuning. Expectedly, this issue was stronger in the fully-sequential case.

Hypothesis 6: Freezing backbone layers can improve BN models, but also their BN-free counterparts. As argued before, the trade-off between sequence length and batch diversity is a disadvantage of BN-based models. By freezing parts of the CNN backbones, sequence lengths can be increased while maintaining the same number of sequences. Hence, we freeze the bottom three blocks of all backbones and retrain each model with sequence lengths of 64, 128 and 256. For BN-free models, we choose the *CHT* strategy but resort to *CHE* for the BN model (Fig. 3c).

Through freezing, 4x64-BN finally outperforms the 2-stage SOTA but collapses again with longer sequences while GN models improve. Even FrozenBN matches other BN-free models. Consistent with prior beliefs [25], lack of normalization might be less problematic in shallow models.

Table 3. State of the art in surgical phase recognition on Cholec80 [62] with 32/8/40 split [22, 35]. Scores (mean+std. over videos) which **outperform** or **match** SOTA are highlighted. Simple, end-to-end CNN-LSTMs outperform multi-stage methods with Attention [22, 35] or complex augmentation pipelines [75].

Method	Details	Acc. (relaxed)	Jacc. (relaxed)
SV-RCNet [33]	(E2E/100x10/SWE)	85.3(± 7.3)	-
C3D+LSTM [79]	(2 stages)	85.9(± 7.9)	-
TeCNO [12]	(2 stages)	88.6(± 7.8)	75.1(± 6.9)
TMRNet [35]	(E2E/2 stages)	89.2(± 9.4)	<u>78.9(± 5.8)</u>
TMRNet [35]	(w/ ResNeSt)	90.1(± 7.6)	<u>79.1(± 5.7)</u>
Trans-SVNet [22]	(3 stages)	90.3(± 7.1)	<u>79.3(± 6.6)</u>
Not-E2E [75]	(3 stages)	<u>91.5(± 7.1)</u>	77.2(± 11.1)
<i>Ours (CNN-LSTM)</i>			
Res-BN	(E2E/4x16/SWE)	87.5(± 7.7)	73.1(± 8.5)
	(E2E/4x16/CHE)	90.3(± 7.1)	77.5(± 8.5)
	(frozen/4x64/CHE)	<u>91.3(± 6.9)</u>	<u>79.8(± 9.2)</u>
Res-FrozenBN	(E2E/1x64/CHT)	90.0(± 7.5)	77.3(± 8.5)
	(frozen/1x256/CHT)	92.5(± 5.9)	81.2(± 9.6)
Res-GN	(E2E/1x64/CHT)	<u>91.4(± 7.8)</u>	<u>78.9(± 9.7)</u>
	(frozen/1x256/CHT)	93.1(± 5.4)	80.2(± 11.7)
ConvNeXt	(E2E/1x64/CHT)	92.4(± 6.9)	82.0(± 7.9)
	(frozen/1x256/CHT)	93.5(± 6.5)	82.9(± 10.1)

Hypothesis 7: Simple end-to-end CNN-LSTMs achieve state-of-the-art performance. Finally, we compare our proposed approaches (end-to-end and partial freezing) to the state of the art in phase recognition. We follow previous work [22, 33, 35] and retrain and evaluate on data splits and metrics proposed by the *M2CAI 2016 Challenge* [58, 62]. They propose variants of common metrics with relaxed boundaries, i.e. errors at phase transitions are ignored under certain conditions. Table 3 shows our results.

Training end-to-end with 64-frame batches, the GN model matches the state of the art in both metrics, while no single SOTA model achieves this. FrozenBN performs slightly worse. Through partial freezing, GN and FrozenBN both clearly outperform the state of the art. The ConvNeXt-based models outperform all methods in all metrics. While the newer ConvNeXt backbone is not necessarily comparable to the ResNet backbones, this does indicate that improving visual-feature learning in simple end-to-end approaches might be more effective than designing more complex temporal models on sub-optimal visual features.

Finally, BN-based end-to-end models perform poorly with SV-RCNet’s sliding-window evaluation (SWE) but improve by carrying hidden states (CHE), indicating that previous end-to-end approaches were evaluated poorly. By freezing backbone layers, BN-based CNN-LSTMs also achieve state-of-the-art results and match the 64-frame, end-to-end GN model. Performance of ConvNeXt or 256-frame GN and FrozenBN models is however not reached. This shows that, with careful design, BN models can still be effective. Nevertheless, models without BatchNorm enable simpler and a wider range of training procedures with longer training sequences and ultimately perform better.

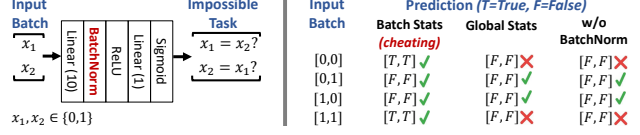


Figure 5. Impossible toy task to illustrate “cheating” with BN: *predicting whether the input is equal to the other sample in the batch*. During training, batch stats can be used to solve the task but the model fails at test time using global stats.

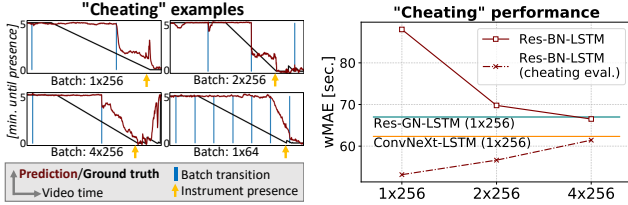
4.3. Anticipation of Instrument Usage

Hypothesis 8: BatchNorm enables “cheating” in certain tasks. BatchNorm can leak information within batches to “cheat” certain objectives. While previous work finds empirical evidence for this effect through degrading performance [68], we conclusively demonstrate it by carefully designing a toy task. Specifically, we propose an impossible task which cannot be solved without “cheating”: *Given training batches of size 2, predict for each input sample whether it is equal to the other sample in the batch*. We use a small neural network with BatchNorm (Fig. 5, left) and with single binary inputs $x_i \in \{0, 1\}$. Although this task is obviously unsolvable when each sample in the batch is processed individually, the BN model “cheats” by making predictions based on batch statistics (Fig. 5, right). Models expectedly fail (always predict *False*) when using global statistics during inference or networks without BN.

Hypothesis 9: “Cheating” can cause BN models to fail in instrument anticipation. To visualize how BN can “cheat” during training in anticipation tasks, we evaluate BN in training mode, i.e. processing test videos offline in batches with sequence lengths equal to the training lengths and use batch (instead of global) statistics for normalization. The effect was most pronounced with sequences similar to the anticipation horizon (5min), so we opt for partial freezing with training sequences of 256 frames (4min16s).

Fig. 6a shows how anticipation predictions immediately improve in batches which contain an instrument occurrence at some point later in the batch. These examples visualize the “cheating” effect explicitly, not only indirectly through impact on performance. Likely, the model has learned to recognize the instrument and the change in feature activations becomes visible to previous frames through batch statistics. Namely, a sudden decrease of activations related to an instrument indicates that a higher mean was subtracted during normalization, so the instrument’s occurrence later in the batch can be inferred. Interestingly, this effect is still visible (but less pronounced) in models trained on batches that contain multiple (4×256) or shorter (1×64) sequences.

In Fig. 6b, we investigate how the “cheating” phenomenon affects anticipation performance. BN models are evaluated either using batch statistics (*cheating eval.*) or using global statistics, which would be the correct approach



(a) Cheating examples (b) Cheating impairs BN models

Figure 6. *Anticipation*: (a) During training, BN models “cheat” by detecting instruments in later frames through batch stats. We visualize this by using batch stats at test time. “Cheating” still happens in batches with multiple or short sequences. (b) By using batch stats at test time, BN models achieve overly good scores (*cheating eval.*) but fail in a fair evaluation. Sampling multiple sequences per batch reduces but does not eliminate the effect.

as future information is generally not available in an online anticipation setting. By using batch statistics at test time, the “cheating” model strongly (but unfairly) outperforms even BN-free end-to-end models. However, we can see that a stronger “cheating” effect (i.e. a lower error with *cheating eval.*, dotted line) leads to a higher error during correct evaluation (solid line). By sampling multiple sequences per batch (4×256), this effect is reduced and the BN model matches the performance of its GN counterpart. However, the gap between the two curves suggests that the model is still learning subpar features due to “cheating”.

Hypothesis 10: End-to-end models outperform state of the art in anticipation. Finally, we compare different models and training strategies to previous work in instrument anticipation [50, 77]. In Table 4, we observe that ConvNeXt and FrozenBN outperform previous work. The GN model only performs well when trained completely end-to-end but gives poor results with partial CNN freezing. As expected, BN models completely fail with fully-sequential batches (1×64 , 1×256) but also provide subpar performance with multiple long sequences (2×256 , 4×256 , 4×64). Likely, this is in part caused by BN’s “cheating” (see Fig. 6a). However, other factors may have contributed since the partially frozen GN model underperforms as well. The end-to-end BN model trained on shorter 16-frame sequences performs surprisingly well. Likely, 16-second batches are too short for effective “cheating”.

Across backbones, complete end-to-end training is more effective than freezing layers, possibly because anticipation is a more challenging task and requires more finetuning of CNN weights. Also, the CHE strategy outperforms CHT in this task. Presumably, the correlation between subsequent batches (and thus SGD steps) is not ideal for this more difficult task. Similarly, FrozenBN models underperformed in the CHT setting in phase recognition (Fig. 3b, 4). Nevertheless, we provide strong evidence for the effectiveness of end-to-end learning also for anticipation and show that BN

Table 4. Comparison of anticipation methods. Scores (mean+std. over runs) which outperform state of the art are highlighted (**bold**)

Anticipation error ↓ (wMAE in sec.)				
SOTA	End-to-end AlexNet-LSTM [50]			66.02(±0.85)
	2-stage ResNet-TCN [77] (variant with only visual features)			65.34(±0.59)
CNN-LSTM:		Res-BN	Res-FrozenBN	Res-GN
2-stage		65.54(±0.21)	-	66.54(±0.31)
E2E	1x64, CHT	-	66.36(±1.30)	67.18(±1.39)
	1x64, CHE	83.78(±3.29)	62.10(±0.06)	64.36(±0.28)
	4x16, CHE	62.06(±0.95)	-	-
frozen	1x256, CHE	88.02(±16.58)	63.10(±0.31)	67.00(±0.87)
	2x256, CHE	69.78(±0.69)	-	-
	4x256, CHE	66.52(±0.51)	-	-
	4x64, CHE	65.30(±0.50)	-	-

models are limited to short sequences and require careful engineering due to the “cheating” phenomenon.

5. Scope and Limitations

Our experiments focus on 2D backbones, due to limitations in the surgical domain, and LSTMs, to show the effectiveness of simple, state-based end-to-end models for online tasks. While the incompatibility of BN and sequential batches is general to the video setting, investigating the feasibility and effectiveness of end-to-end approaches for other domains, backbones and temporal models requires further work and falls outside the scope of our study. Liu et al. [42] recently provided an extensive, insightful study on end-to-end temporal action detection with a wider range of models. However, BN issues are not discussed, although the common FrozenBN solution is utilized. Our work, on the other hand, specifically aims at providing a deeper understanding of BN’s limitations in long-video settings but restricts practical implications to a smaller range of models.

6. Conclusion

We investigate the limitations of BatchNorm for end-to-end video learning, which are especially relevant in surgical workflow tasks where CNN backbones require finetuning. In a detailed literature review, we reveal how research has circumvented these problems by moving towards complex, multi-stage approaches. We identify situations where BN models fail and how it affects end-to-end training strategies. Specifically, BN restricts the length of training sequences and in online settings, can interfere with hidden-state handling of LSTMs as well as leak information from future frames. We show that the latter can be used by models to “cheat” in anticipation tasks. We also find that the common ad-hoc solution FrozenBN is only effective in restricted settings. Instead, even simple CNN-LSTMs reach the state of the art in two SWA tasks by avoiding BatchNorm entirely.

Although limitations of BN have been discussed before, we believe a comprehensive and deeper understanding in the long-video context is crucial for future research in surgical workflow analysis. End-to-end learning is favorable

over multi-stage approaches but we hypothesize that BN issues have silently hidden its advantages. Moving forward, the field could benefit from reconsidering end-to-end approaches and further investigating BN-free backbones. In natural-video tasks like action segmentation, where end-to-end learning currently plays only a minor role, re-evaluating training strategies could potentially be valuable as well.

Acknowledgements Funded by the German Research Foundation (DFG, Deutsche Forschungsgemeinschaft) as part of Germany’s Excellence Strategy – EXC 2050/1 – Project ID 390696704 – Cluster of Excellence “Centre for Tactile Internet with Human-in-the-Loop” (CeTI) of Technische Universität Dresden.

References

- [1] Yazan Abu Farha, Qihong Ke, Bernt Schiele, and Juergen Gall. Long-term anticipation of activities with cycle consistency. In *DAGM German Conference on Pattern Recognition*, pages 159–173. Springer, 2020. 1, 3
- [2] Ivan Aksamentov, Andru Putra Twinanda, Didier Mutter, Jacques Marescaux, and Nicolas Padoy. Deep neural networks predict remaining surgery duration from cholecystectomy videos. In *International Conference on Medical Image Computing and Computer-Assisted Intervention*, pages 586–593. Springer, 2017. 2, 3, 4
- [3] Mathieu Andreux, Jean Ogier du Terrail, Constance Beguier, and Eric W Tramel. Siloed federated learning for multi-centric histopathology datasets. In *Domain Adaptation and Representation Transfer, and Distributed and Collaborative Learning*, pages 129–139. Springer, 2020. 2
- [4] Jimmy Lei Ba, Jamie Ryan Kiros, and Geoffrey E Hinton. Layer normalization. *arXiv preprint arXiv:1607.06450*, 2016. 1, 2, 4
- [5] Sophia Bano, Francisco Vasconcelos, Emmanuel Van der Poorten, Tom Vercauteren, Sebastien Ourselin, Jan Deprest, and Danail Stoyanov. Fetnet: a recurrent convolutional network for occlusion identification in fetoscopic videos. *International journal of computer assisted radiology and surgery*, 15(5):791–801, 2020. 1, 3
- [6] Nils Bjorck, Carla P Gomes, Bart Selman, and Kilian Q Weinberger. Understanding batch normalization. *Advances in neural information processing systems*, 31, 2018. 2
- [7] Sebastian Bodenstedt, Dominik Rivoir, Alexander Jenke, Martin Wagner, Michael Breucha, Beat Müller-Stich, Sören Torge Mees, Jürgen Weitz, and Stefanie Speidel. Active learning using deep bayesian networks for surgical workflow analysis. *International journal of computer assisted radiology and surgery*, 14(6):1079–1087, 2019. 2, 3
- [8] Sebastian Bodenstedt, Martin Wagner, Lars Mündermann, Hannes Kenngott, Beat Müller-Stich, Michael Breucha, Sören Torge Mees, Jürgen Weitz, and Stefanie Speidel. Prediction of laparoscopic procedure duration using unlabeled, multimodal sensor data. *International Journal of Computer Assisted Radiology and Surgery*, 14(6):1089–1095, 2019. 3
- [9] Andy Brock, Soham De, Samuel L Smith, and Karen Simonyan. High-performance large-scale image recognition without normalization. In *International Conference on Machine Learning*, pages 1059–1071. PMLR, 2021. 1, 2
- [10] Dongqi Cai, Anbang Yao, and Yurong Chen. Dynamic normalization and relay for video action recognition. *Advances in neural information processing systems*, 34:11026–11040, 2021. 1, 2, 6
- [11] Joao Carreira and Andrew Zisserman. Quo vadis, action recognition? a new model and the kinetics dataset. In *proceedings of the IEEE Conference on Computer Vision and Pattern Recognition*, pages 6299–6308, 2017. 1, 3
- [12] Tobias Czempiel, Magdalini Paschali, Matthias Keicher, Walter Simson, Hubertus Feussner, Seong Tae Kim, and Nassir Navab. Tecno: Surgical phase recognition with multi-stage temporal convolutional networks. In *International conference on medical image computing and computer-assisted intervention*, pages 343–352. Springer, 2020. 1, 2, 3, 4, 5, 6, 7, 13, 14, 16, 17
- [13] Tobias Czempiel, Magdalini Paschali, Daniel Ostler, Seong Tae Kim, Benjamin Busam, and Nassir Navab. Opera: Attention-regularized transformers for surgical phase recognition. In *International Conference on Medical Image Computing and Computer-Assisted Intervention*, pages 604–614. Springer, 2021. 2, 3, 4
- [14] Tobias Czempiel, Aidean Sharghi, Magdalini Paschali, and Omid Mohareri. Surgical workflow recognition: from analysis of challenges to architectural study. *arXiv preprint arXiv:2203.09230*, 2022. 1, 3
- [15] Soham De and Sam Smith. Batch normalization biases residual blocks towards the identity function in deep networks. *Advances in Neural Information Processing Systems*, 33:19964–19975, 2020. 2
- [16] Alexey Dosovitskiy, Lucas Beyer, Alexander Kolesnikov, Dirk Weissenborn, Xiaohua Zhai, Thomas Unterthiner, Mostafa Dehghani, Matthias Minderer, Georg Heigold, Sylvain Gelly, et al. An image is worth 16x16 words: Transformers for image recognition at scale. *arXiv preprint arXiv:2010.11929*, 2020. 2
- [17] Hyunjun Eun, Jinyoung Moon, Jongyoul Park, Chanho Jung, and Changick Kim. Learning to discriminate information for online action detection. In *Proceedings of the IEEE/CVF Conference on Computer Vision and Pattern Recognition*, pages 809–818, 2020. 3
- [18] Yazan Abu Farha and Jurgen Gall. Ms-ten: Multi-stage temporal convolutional network for action segmentation. In *Proceedings of the IEEE/CVF Conference on Computer Vision and Pattern Recognition*, pages 3575–3584, 2019. 1, 3
- [19] Alireza Fathi, Xiaofeng Ren, and James M Rehg. Learning to recognize objects in egocentric activities. In *CVPR 2011*, pages 3281–3288. IEEE, 2011. 5, 13, 15
- [20] Antonino Furnari and Giovanni Maria Farinella. Rolling-unrolling lstms for action anticipation from first-person video. *IEEE transactions on pattern analysis and machine intelligence*, 43(11):4021–4036, 2020. 3, 4
- [21] Jiyang Gao, Zhenheng Yang, and Ram Nevatia. Red: Reinforced encoder-decoder networks for action anticipation. *arXiv preprint arXiv:1707.04818*, 2017. 3, 4

- [22] Xiaojie Gao, Yueming Jin, Yonghao Long, Qi Dou, and Pheng-Ann Heng. Trans-svnet: accurate phase recognition from surgical videos via hybrid embedding aggregation transformer. In *International Conference on Medical Image Computing and Computer-Assisted Intervention*, pages 593–603. Springer, 2021. 1, 2, 3, 4, 5, 7, 16
- [23] Reza Ghoddoosian, Isht Dwivedi, Nakul Agarwal, Chiho Choi, and Behzad Dariush. Weakly-supervised online action segmentation in multi-view instructional videos. In *Proceedings of the IEEE/CVF Conference on Computer Vision and Pattern Recognition*, pages 13780–13790, 2022. 3, 4
- [24] Rohit Girdhar and Kristen Grauman. Anticipative video transformer. In *Proceedings of the IEEE/CVF International Conference on Computer Vision*, pages 13505–13515, 2021. 3
- [25] Kaiming He, Xiangyu Zhang, Shaoqing Ren, and Jian Sun. Deep residual learning for image recognition. In *Proceedings of the IEEE conference on computer vision and pattern recognition*, pages 770–778, 2016. 1, 6
- [26] Olivier Henaff. Data-efficient image recognition with contrastive predictive coding. In *International Conference on Machine Learning*, pages 4182–4192. PMLR, 2020. 2
- [27] Sepp Hochreiter and Jürgen Schmidhuber. Long short-term memory. *Neural computation*, 9(8):1735–1780, 1997. 1
- [28] Elad Hoffer, Itay Hubara, and Daniel Soudry. Train longer, generalize better: closing the generalization gap in large batch training of neural networks. *Advances in neural information processing systems*, 30, 2017. 2
- [29] Yifei Huang, Yusuke Sugano, and Yoichi Sato. Improving action segmentation via graph-based temporal reasoning. In *Proceedings of the IEEE/CVF conference on computer vision and pattern recognition*, pages 14024–14034, 2020. 1, 3
- [30] Sergey Ioffe. Batch renormalization: Towards reducing minibatch dependence in batch-normalized models. *Advances in neural information processing systems*, 30, 2017. 2
- [31] Sergey Ioffe and Christian Szegedy. Batch normalization: Accelerating deep network training by reducing internal covariate shift. In *International conference on machine learning*, pages 448–456. PMLR, 2015. 1, 2
- [32] Yuchi Ishikawa, Seito Kasai, Yoshimitsu Aoki, and Hirokatsu Kataoka. Alleviating over-segmentation errors by detecting action boundaries. In *Proceedings of the IEEE/CVF Winter Conference on Applications of Computer Vision*, pages 2322–2331, 2021. 1, 3
- [33] Yueming Jin, Qi Dou, Hao Chen, Lequan Yu, Jing Qin, Chi-Wing Fu, and Pheng-Ann Heng. Sv-rcnet: workflow recognition from surgical videos using recurrent convolutional network. *IEEE transactions on medical imaging*, 37(5):1114–1126, 2017. 1, 3, 4, 5, 7
- [34] Yueming Jin, Huaxia Li, Qi Dou, Hao Chen, Jing Qin, Chi-Wing Fu, and Pheng-Ann Heng. Multi-task recurrent convolutional network with correlation loss for surgical video analysis. *Medical image analysis*, 59:101572, 2020. 2, 3
- [35] Yueming Jin, Yonghao Long, Cheng Chen, Zixu Zhao, Qi Dou, and Pheng-Ann Heng. Temporal memory relation network for workflow recognition from surgical video. *IEEE Transactions on Medical Imaging*, 40(7):1911–1923, 2021. 2, 3, 7, 16
- [36] Siddharth Kannan, Gaurav Yengera, Didier Mutter, Jacques Marescaux, and Nicolas Padoy. Future-state predicting lstm for early surgery type recognition. *IEEE Transactions on Medical Imaging*, 39(3):556–566, 2019. 1, 2, 3
- [37] Qihong Ke, Mario Fritz, and Bernt Schiele. Time-conditioned action anticipation in one shot. In *Proceedings of the IEEE/CVF Conference on Computer Vision and Pattern Recognition*, pages 9925–9934, 2019. 1, 3
- [38] Alex Krizhevsky, Ilya Sutskever, and Geoffrey E Hinton. Imagenet classification with deep convolutional neural networks. In F. Pereira, C. J. C. Burges, L. Bottou, and K. Q. Weinberger, editors, *Advances in Neural Information Processing Systems*, volume 25. Curran Associates, Inc., 2012. 3, 4
- [39] Antoine Labatie, Dominic Masters, Zach Eaton-Rosen, and Carlo Luschi. Proxy-normalizing activations to match batch normalization while removing batch dependence. *Advances in Neural Information Processing Systems*, 34, 2021. 2
- [40] Colin Lea, Michael D. Flynn, Rene Vidal, Austin Reiter, and Gregory D. Hager. Temporal convolutional networks for action segmentation and detection. In *Proceedings of the IEEE Conference on Computer Vision and Pattern Recognition (CVPR)*, July 2017. 3
- [41] Hanxiao Liu, Andy Brock, Karen Simonyan, and Quoc Le. Evolving normalization-activation layers. *Advances in Neural Information Processing Systems*, 33:13539–13550, 2020. 2
- [42] Xiaolong Liu, Song Bai, and Xiang Bai. An empirical study of end-to-end temporal action detection. In *Proceedings of the IEEE/CVF Conference on Computer Vision and Pattern Recognition*, pages 20010–20019, 2022. 3, 4, 8
- [43] Zhuang Liu, Hanzi Mao, Chao-Yuan Wu, Christoph Feichtenhof, Trevor Darrell, and Saining Xie. A convnet for the 2020s. *arXiv preprint arXiv:2201.03545*, 2022. 2, 4
- [44] Lena Maier-Hein, Matthias Eisenmann, Duygu Sarikaya, Keno März, Toby Collins, Anand Malpani, Johannes Fallert, Hubertus Feussner, Stamatia Giannarou, Pietro Mascagni, et al. Surgical data science—from concepts toward clinical translation. *Medical image analysis*, 76:102306, 2022. 2
- [45] Lena Maier-Hein, Swaroop S Vedula, Stefanie Speidel, Nasir Navab, Ron Kikinis, Adrian Park, Matthias Eisenmann, Hubertus Feussner, Germain Forestier, Stamatia Giannarou, et al. Surgical data science for next-generation interventions. *Nature Biomedical Engineering*, 1(9):691–696, 2017. 2
- [46] Andrés Marafioti, Michel Hayoz, Mathias Gallardo, Pablo Márquez Neila, Sebastian Wolf, Martin Zinkernagel, and Raphael Sznitman. Catanet: Predicting remaining cataract surgery duration. In *International Conference on Medical Image Computing and Computer-Assisted Intervention*, pages 426–435. Springer, 2021. 1, 2, 3, 4
- [47] Chinedu Innocent Nwoye, Didier Mutter, Jacques Marescaux, and Nicolas Padoy. Weakly supervised convolutional lstm approach for tool tracking in laparoscopic videos. *International journal of computer assisted radiology and surgery*, 14(6):1059–1067, 2019. 2, 3, 4

- [48] Quang Pham, Chenghao Liu, and Steven Hoi. Continual normalization: Rethinking batch normalization for online continual learning. *arXiv preprint arXiv:2203.16102*, 2022. **2**
- [49] Dominik Rivoir, Sebastian Bodenstedt, Felix von Bechtolsheim, Marius Distler, Jürgen Weitz, and Stefanie Speidel. Unsupervised temporal video segmentation as an auxiliary task for predicting the remaining surgery duration. In *OR 2.0 Context-Aware Operating Theaters and Machine Learning in Clinical Neuroimaging*, pages 29–37. Springer, 2019. **3**
- [50] Dominik Rivoir, Sebastian Bodenstedt, Isabel Funke, Felix von Bechtolsheim, Marius Distler, Jürgen Weitz, and Stefanie Speidel. Rethinking anticipation tasks: Uncertainty-aware anticipation of sparse surgical instrument usage for context-aware assistance. In *International Conference on Medical Image Computing and Computer-Assisted Intervention*, pages 752–762. Springer, 2020. **1, 2, 3, 5, 8, 14, 15, 16**
- [51] Tim Salimans and Durk P Kingma. Weight normalization: A simple reparameterization to accelerate training of deep neural networks. *Advances in neural information processing systems*, 29, 2016. **2**
- [52] Fadime Sener, Dipika Singhania, and Angela Yao. Temporal aggregate representations for long-range video understanding. In *European Conference on Computer Vision*, pages 154–171. Springer, 2020. **1, 3**
- [53] Sheng Shen, Zhewei Yao, Amir Gholami, Michael Mahoney, and Kurt Keutzer. Powernorm: Rethinking batch normalization in transformers. In *International Conference on Machine Learning*, pages 8741–8751. PMLR, 2020. **1, 2**
- [54] Xueying Shi, Yueming Jin, Qi Dou, and Pheng-Ann Heng. Lrtd: long-range temporal dependency based active learning for surgical workflow recognition. *International Journal of Computer Assisted Radiology and Surgery*, 15(9):1573–1584, 2020. **2, 3**
- [55] Karen Simonyan and Andrew Zisserman. Very deep convolutional networks for large-scale image recognition. *arXiv preprint arXiv:1409.1556*, 2014. **3**
- [56] Saurabh Singh and Shankar Krishnan. Filter response normalization layer: Eliminating batch dependence in the training of deep neural networks. In *Proceedings of the IEEE/CVF Conference on Computer Vision and Pattern Recognition*, pages 11237–11246, 2020. **2**
- [57] Saurabh Singh and Abhinav Shrivastava. Evalnorm: Estimating batch normalization statistics for evaluation. In *Proceedings of the IEEE/CVF International Conference on Computer Vision*, pages 3633–3641, 2019. **2**
- [58] Ralf Stauder, Daniel Ostler, Michael Krantzfeld, Sebastian Koller, Hubertus Feußner, and Nassir Navab. The tum lapc-hole dataset for the m2cai 2016 workflow challenge. *arXiv preprint arXiv:1610.09278*, 2016. **7, 16**
- [59] Sebastian Stein and Stephen J McKenna. Combining embedded accelerometers with computer vision for recognizing food preparation activities. In *Proceedings of the 2013 ACM international joint conference on Pervasive and ubiquitous computing*, pages 729–738, 2013. **5, 13, 14, 15**
- [60] Christian Szegedy, Vincent Vanhoucke, Sergey Ioffe, Jon Shlens, and Zbigniew Wojna. Rethinking the inception architecture for computer vision. In *Proceedings of the IEEE conference on computer vision and pattern recognition*, pages 2818–2826, 2016. **1**
- [61] Mingxing Tan and Quoc Le. Efficientnet: Rethinking model scaling for convolutional neural networks. In *International conference on machine learning*, pages 6105–6114. PMLR, 2019. **1**
- [62] Andru P Twinanda, Sherif Shehata, Didier Mutter, Jacques Marescaux, Michel De Mathelin, and Nicolas Padoy. Endonet: a deep architecture for recognition tasks on laparoscopic videos. *IEEE transactions on medical imaging*, 36(1):86–97, 2016. **1, 2, 3, 5, 7, 14, 15**
- [63] Andru Putra Twinanda, Gaurav Yengera, Didier Mutter, Jacques Marescaux, and Nicolas Padoy. Rsdnet: Learning to predict remaining surgery duration from laparoscopic videos without manual annotations. *IEEE transactions on medical imaging*, 38(4):1069–1078, 2018. **2, 3**
- [64] Dmitry Ulyanov, Andrea Vedaldi, and Victor Lempitsky. Instance normalization: The missing ingredient for fast stylization. *arXiv preprint arXiv:1607.08022*, 2016. **2**
- [65] Ashish Vaswani, Noam Shazeer, Niki Parmar, Jakob Uszkoreit, Llion Jones, Aidan N Gomez, Łukasz Kaiser, and Illia Polosukhin. Attention is all you need. *Advances in neural information processing systems*, 30, 2017. **1, 2**
- [66] Zhenzhi Wang, Ziteng Gao, Limin Wang, Zhifeng Li, and Gangshan Wu. Boundary-aware cascade networks for temporal action segmentation. In *European Conference on Computer Vision*, pages 34–51. Springer, 2020. **1, 3**
- [67] Yuxin Wu and Kaiming He. Group normalization. In *Proceedings of the European conference on computer vision (ECCV)*, pages 3–19, 2018. **1, 2, 4, 5, 6, 13**
- [68] Yuxin Wu and Justin Johnson. Rethinking” batch” in batch-norm. *arXiv preprint arXiv:2105.07576*, 2021. **1, 2, 4, 5, 7**
- [69] Mingze Xu, Mingfei Gao, Yi-Ting Chen, Larry S Davis, and David J Crandall. Temporal recurrent networks for online action detection. In *Proceedings of the IEEE/CVF International Conference on Computer Vision*, pages 5532–5541, 2019. **3**
- [70] Junjie Yan, Ruosi Wan, Xiangyu Zhang, Wei Zhang, Yichen Wei, and Jian Sun. Towards stabilizing batch statistics in backward propagation of batch normalization. *arXiv preprint arXiv:2001.06838*, 2020. **2**
- [71] Xinyu Yang, Majid Mirmehdi, and Tilo Burghardt. Back to the future: Cycle encoding prediction for self-supervised video representation learning. In *The 32nd British Machine Vision Conference*, 2021. **2**
- [72] Zhuliang Yao, Yue Cao, Yutong Lin, Ze Liu, Zheng Zhang, and Han Hu. Leveraging batch normalization for vision transformers. In *Proceedings of the IEEE/CVF International Conference on Computer Vision*, pages 413–422, 2021. **4**
- [73] Zhuliang Yao, Yue Cao, Shuxin Zheng, Gao Huang, and Stephen Lin. Cross-iteration batch normalization. In *Proceedings of the IEEE/CVF conference on computer vision and pattern recognition*, pages 12331–12340, 2021. **2, 6**
- [74] Gaurav Yengera, Didier Mutter, Jacques Marescaux, and Nicolas Padoy. Less is more: Surgical phase recognition

with less annotations through self-supervised pre-training of cnn-lstm networks. *arXiv preprint arXiv:1805.08569*, 2018. 3, 14

- [75] Fangqiu Yi and Tingting Jiang. Not end-to-end: Explore multi-stage architecture for online surgical phase recognition. In *Proceedings of the Asian Conference on Computer Vision*, 2022. 2, 3, 4, 7
- [76] Fangqiu Yi, Hongyu Wen, and Tingting Jiang. Asformer: Transformer for action segmentation. In *The British Machine Vision Conference (BMVC)*, 2021. 1, 3
- [77] Kun Yuan, Matthew Holden, Shijian Gao, and Won-Sook Lee. Surgical workflow anticipation using instrument interaction. In *International conference on medical image computing and computer-assisted intervention*, pages 615–625. Springer, 2021. 1, 2, 3, 4, 8, 16
- [78] Bokai Zhang, Amer Ghanem, Alexander Simes, Henry Choi, Andrew Yoo, and Andrew Min. Swnet: Surgical workflow recognition with deep convolutional network. In *Medical Imaging with Deep Learning*, pages 855–869. PMLR, 2021. 3
- [79] Yitong Zhang, Sophia Bano, Ann-Sophie Page, Jan De-prest, Danail Stoyanov, and Francisco Vasconcelos. Large-scale surgical workflow segmentation for laparoscopic sacrocolpopexy. *International Journal of Computer Assisted Radiology and Surgery*, pages 1–11, 2022. 1, 2, 3, 4, 7
- [80] Peisen Zhao, Lingxi Xie, Ya Zhang, Yanfeng Wang, and Qi Tian. Privileged knowledge distillation for online action detection. *arXiv preprint arXiv:2011.09158*, 2020. 3
- [81] Odysseas Zisimopoulos, Evangello Flouty, Imanol Luengo, Petros Giataganas, Jean Nehme, Andre Chow, and Danail Stoyanov. Deepphase: surgical phase recognition in cataracts videos. In *International conference on medical image computing and computer-assisted intervention*, pages 265–272. Springer, 2018. 2, 3, 4

A. Results for Surgical Phase Recognition

Tables 5 and 6 provide an overview of accuracy and F1 scores for surgical phase recognition. The accuracy scores were presented in the form of figures in the main paper.

Table 5. Accuracy scores (mean + sample std. over runs) for surgical phase recognition on TeCNO’s [12] split (40 train. videos, 8 val., 32 test) used for our main analysis. Per run, accuracy is computed per video and then averaged. We **highlight** scores which outperform all 2-stage approaches by at least its sample standard deviation. Note that these results were presented in the form of figures in the main paper

	Accuracy (video-wise) ↑			
	BN	FrozenBN	GN	ConvNeXt
2-Stage				
LSTM	89.1(±0.5)	-	87.2(±0.7)	87.8(±0.3)
TCN (*TeCNO reimpl.)	*89.4(±0.8)	-	88.4(±0.8)	88.2(±0.1)
TeCNO [12] (original)	88.56(±0.27)	-	-	-
End-to-end				
8 × 8, sliding eval.	85.9(±0.1)	85.2(±0.6)	83.0(±2.2)	85.9(±0.2)
4 × 16, sliding eval.	86.5(±1.4)	86.1(±1.2)	85.8(±0.7)	88.0(±0.9)
2 × 32, sliding eval.	86.5(±0.4)	86.5(±1.2)	87.5(±2.3)	87.9(±0.5)
1 × 64, sliding eval.	57.2(±4.2)	88.4(±1.9)	88.4(±0.8)	89.3(±1.2)
8 × 8, carry-hidden eval.	89.4(±0.4)	89.0(±0.4)	86.8(±1.3)	88.1(±0.2)
4 × 16, carry-hidden eval.	89.6(±1.0)	89.4(±1.0)	87.9(±0.8)	89.1(±1.1)
2 × 32, carry-hidden eval.	88.2(±0.7)	89.4(±1.0)	88.9(±2.3)	88.6(±0.6)
1 × 64, carry-hidden eval.	59.7(±3.8)	89.6(±1.1)	89.3(±0.4)	89.5(±1.1)
1 × 64, carry-hidden train.	55.6(±3.1)	89.4(±0.4)	90.5(±0.9)	92.3(±1.5)
Partially frozen				
4 × 64, carry-hidden eval.	90.1(±2.2)	-	-	-
2 × 128, carry-hidden eval.	88.5(±1.6)	-	-	-
1 × 256, carry-hidden eval.	76.7(±1.5)	-	-	-
1 × 64, carry-hidden train.	-	92.4(±0.4)	89.7(±1.8)	93.3(±0.3)
1 × 128, carry-hidden train.	-	92.0(±0.5)	92.3(±0.5)	92.5(±1.2)
1 × 256, carry-hidden train.	-	92.1(±0.4)	92.6(±0.5)	92.6(±0.1)

Table 6. F1 scores (mean + sample std. over runs) for surgical phase recognition on TeCNO’s [12] split (40 train. videos, 8 val., 32 test) used for our main analysis. Per training run, we compute the frame-based confusion matrix over the entire test set, compute a single F1 score per phase and average over phases. This strategy deviates from video-wise approaches in previous work but is less ambiguous and gives smoother scores in edge cases. We **highlight** scores which outperform all 2-stage approaches by at least its sample standard deviation

	F1 (frame-wise) ↑			
	BN	FrozenBN	GN	ConvNeXt
2-Stage				
LSTM	83.2(±0.9)	-	80.2(±1.2)	81.0(±0.2)
TCN	83.4(±1.2)	-	81.0(±1.0)	81.7(±0.6)
End-to-end				
8 × 8, sliding eval.	79.3(±0.9)	78.8(±0.2)	74.6(±2.1)	78.4(±1.2)
4 × 16, sliding eval.	80.4(±1.7)	80.4(±0.8)	78.8(±0.7)	82.3(±1.0)
2 × 32, sliding eval.	79.1(±0.9)	81.1(±0.5)	81.5(±2.7)	81.9(±1.3)
1 × 64, sliding eval.	36.3(±3.1)	83.2(±1.4)	81.8(±0.7)	84.0(±1.0)
8 × 8, carry-hidden eval.	83.2(±1.0)	82.8(±0.8)	79.4(±0.8)	81.9(±0.6)
4 × 16, carry-hidden eval.	83.6(±1.6)	83.2(±0.9)	81.5(±0.5)	83.7(±1.2)
2 × 32, carry-hidden eval.	81.3(±0.9)	82.8(±1.1)	82.9(±2.9)	83.2(±0.8)
1 × 64, carry-hidden eval.	37.1(±3.0)	82.8(±1.9)	82.9(±0.5)	84.5(±0.9)
1 × 64, carry-hidden train.	40.0(±4.1)	82.2(±0.2)	83.9(±0.7)	86.2(±1.7)
Partially frozen				
4 × 64, carry-hidden eval.	84.5(±1.4)	-	-	-
2 × 128, carry-hidden eval.	79.8(±2.6)	-	-	-
1 × 256, carry-hidden eval.	58.8(±0.9)	-	-	-
1 × 64, carry-hidden train.	-	85.3(±1.3)	82.4(±1.0)	87.4(±0.7)
1 × 128, carry-hidden train.	-	85.0(±0.5)	83.8(±1.7)	87.5(±0.9)
1 × 256, carry-hidden train.	-	85.5(±0.6)	84.8(±0.4)	87.1(±0.5)

Table 7. FrozenBN models exhibit more instability during training than GN models. Initial learning rates of FrozenBN models often had to be reduced in order to prevent model collapse (red), but higher learning rates were preferable in cases without collapse.

Learning rate	Accuracy (video-wise) ↑			
	FrozenBN		GN	
	E2E/1x64			
	CHE	CHT	CHE	CHT
10 ⁻⁶	88.2(±0.1)	89.4(±0.4)	83.7(±2.3)	88.4(±0.2)
10 ⁻⁵	89.6(±1.1)	39.8(±0.0)	89.3(±0.4)	90.5(±0.9)
	frozen/1x256			
	CHE	CHT	CHE	CHT
10 ⁻⁵	90.0(±0.7)	92.1(±0.4)	86.9(±0.5)	89.5(±0.7)
10 ⁻⁴	39.8(±0.0)	39.8(±0.0)	91.1(±0.9)	92.6(±0.5)

Table 8. Accuracy scores for *online* action segmentation on the GTEA dataset [19]. We use the suggested splits for 4-fold cross validation. Note that most works propose offline methods. For each backbone, we **highlight** the training strategy (CHE vs. CHT) which performs better. Note that these results were presented in the form of a bar plot in the main paper.

GTEA				
	Accuracy (video-wise) ↑			
	BN	FrozenBN	GN	ConvNeXt
2-Stage				
LSTM	60.1	-	-	-
TCN	63.2	-	-	-
End-to-end, 1 × 64				
CHE	-	66.6	63.9	63.5
CHT	43.6	64.3	66.8	68.9

In Table 7, we provide additional evidence that models with FrozenBN exhibit more instability during training.

B. Results for Online Action Segmentation

Tables 8 and 9 show our results on the GTEA [19] and 50Salads [59] datasets. These are the same results which were presented in form of a bar plot in the paper. Differently from most previous work, we formulate action segmentation as an online task on these datasets. We use the suggested splits for K-fold cross validation but for each training run, we use one set for validation (model selection), one set for testing and the remaining for training. We use the same hyperparameters as for surgical phase recognition (see Sec. E).

C. Model Architectures

Fig. 7 shows the network architectures used in our experiments. For the GroupNorm-based Resnet-50, we use GroupNorm with 32 groups since this performed best in the original paper [67] and has a pretrained model available¹. For 2-stage TCN models, we follow TeCNO [12] as close as possible. Although not reported in the paper, we follow

¹<https://github.com/ppwyyxx/GroupNorm-reproduce/releases/tag/v0.1>

Table 9. Accuracy scores for *online* action segmentation on the *50Salads* dataset [59]. We use the suggested splits for 5-fold cross validation. Note that most works propose offline methods. For each backbone, we **highlight** the training strategy (CHE vs. CHT) which performs better. Note that these results were presented in the form of a bar plot in the main paper.

50Salads				
Accuracy (video-wise) \uparrow				
	BN	FrozenBN	GN	ConvNeXt
2-Stage				
LSTM	69.4	-	-	-
TCN	72.0	-	-	-
End-to-end, 1×64				
CHE	-	77.9	80.4	79.3
CHT	23.5	77.5	83.8	83.3

their exact model configuration with 2 stages, 9 layers per stage and 64 feature channels per layer².

Fig. 8 shows which backbone blocks are frozen in the respective experiments. Note that with a BN-based backbone, batch statistics were still used for normalization during training. Setting BN to evaluation mode in frozen layers led to model failure.

D. Task Formulations

D.1. Surgical Phase Recognition

Surgical phase recognition on the Cholec80 dataset [62] is a dense temporal segmentation task with 7 phases and is therefore a simple multi-class classification when viewed at the frame level. Given a frame x with corresponding class label $c \in \{1, \dots, 7\}$ and a softmax-activated neural network f which outputs a 7D vector per input image, we use the standard cross-entropy loss for optimization:

$$L_{phase}(x, c) = -\log f(x)[c] \quad (1)$$

D.2. Anticipation of Surgical Instrument Usage

For instrument anticipation we follow the task formulation from previous work [50]. We anticipate 5 different instruments on the Cholec80 dataset, where the main task is to predict the remaining duration until occurrence of each instrument at each time point up to a horizon of 5 minutes. As an auxiliary classification task, we also predict whether each instrument is present and whether or not it will appear within the next 5 minutes (i.e. inside or outside of horizon).

Given a frame x and the corresponding remaining durations t_i for each instrument $i \in \{1, \dots, 5\}$ and the horizon $h = 5$, the ground-truth value for the main regression task

is defined as

$$y_i = \min(t_i, h). \quad (2)$$

The corresponding ground-truth class for the auxiliary classification task is

$$c_i = \begin{cases} 1, & y_i = 0 \text{ (instrument present)} \\ 2, & 0 < y_i < h \text{ (inside horizon)} \\ 3, & y_i = h \text{ (outside horizon)} \end{cases}. \quad (3)$$

We then jointly optimize both tasks with the SmoothL1 [74] loss for regression and cross entropy for classification:

$$L_{ant}(x, y) = \sum_{i=1}^5 \text{SmoothL1}(f_{reg}^i(x), y_i) - \lambda \log f_{cls}^i(x)[c_i], \quad (4)$$

where f_{reg}^i and f_{cls}^i are the regression and classification predictions of a neural network for instrument i and $\lambda = 0.01$ is a scaling factor for the auxiliary task.

E. Training Details & Hyperparameters

Tables 10, 11 and 12 summarize our training hyperparameters. Some of our choices, especially the differences between training procedures (Table 11), might require clarification:

1. In 'partially frozen' models for phase recognition, we trained for 100 epochs on the 40/8/32 split, but 200 epochs on the 32/8/40 split for state-of-the-art comparison due to the smaller training set. This was only done for efficiency reasons, since 100 epochs seemed to be enough with 40 train videos. The 'partial freezing' models did not deteriorate with longer training duration.
2. When training only the backbone (for 2-stage approaches), we shortened the definition of an epoch, since the CNN overfit too quickly on the image task and would provide bad features for the temporal model in the subsequent stage. In all other scenarios, we sample frames equal to the size of the train set in each epoch.
3. Except for the number of epochs, we use exactly the same settings for phase recognition and anticipation. Convergence was much slower in anticipation.
4. The learning rate for training temporal models only in 2-stage approaches ($5 \cdot 10^{-4}$) was taken from TeCNO [12] and also seemed to perform best in our experiments.

²<https://github.com/tobiascz/TeCNO/issues/6#issuecomment-802851853>

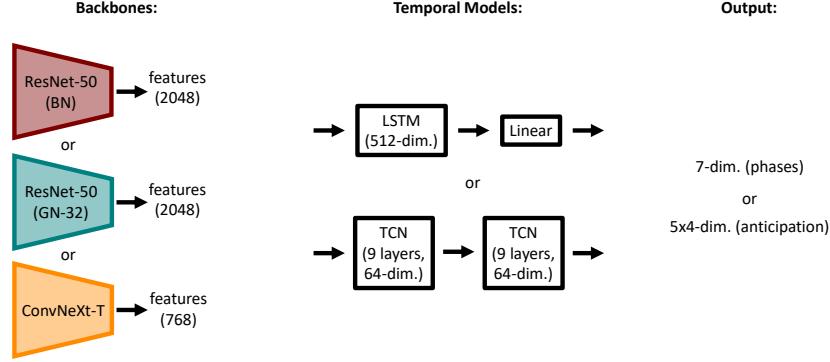


Figure 7. Overview of model architectures used in our experiments. For instrument anticipation, we follow the original task formulation [50]. For each of 5 instruments, 4 prediction values are required (1 for duration prediction and 3 for the auxiliary classification task)

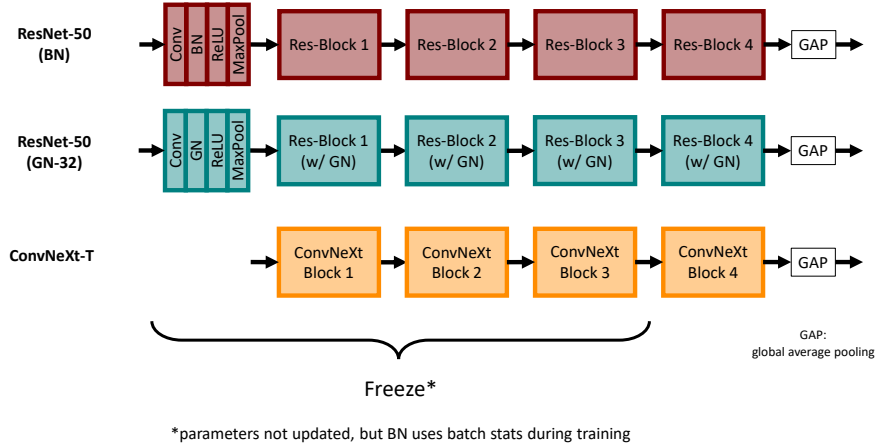


Figure 8. How backbones were frozen in the 'partially frozen' models. Note that with a BN-based backbone, batch statistics were still used for normalization during training. Setting BN to evaluation mode in frozen layers led to model failure

Table 10. Overview of global hyperparameters (used in all settings)

Optimizer	AdamW
Weight decay	0.01
Image size	216 × 384
Data aug.	Shift, Scale, Crop, RGB shift, Brightness shift, Contrast shift

5. Random data augmentations were performed on images individually in all experiments. So, even in sequential batches, different augmentations were done on each frame. This setting performed surprisingly well.

F. Metrics

Metrics can have subtle properties which might lead to misleading scores. Also, even common metrics like accuracies or F1 scores can be computed in many different ways

Table 11. Overview of hyperparameters which depend on the training strategy or task. Action segmentation methods on GTEA and 50Salads use the same hyperparameters as for phase recognition.

Training type	Epochs		Learn. rate	Batch size	Batches per epoch
	Phase	Antic.			
Backbone only	50	300	10^{-5}	32	#frames / 256
Temporal only	100	100	$5 \cdot 10^{-4}$	whole video	#videos
End-to-end	200	300	10^{-5}	64	#frames / batch size
Partially frozen	100*	300	10^{-4}	64,128,256	#frames / batch size

*200 for phase SOTA comparison due to smaller train set

†FrozenBN models which collapsed under these parameters used a reduced learning rate by factor 10 (E2E/CHT, frozen/CHE, frozen/CHT, on Cholec80 and 50Salads)

Table 12. Dataset hyperparameters

	FPS	Image resolution	Classes	Videos
Cholec80 [62]	1	216 × 384	7	80
GTEA [19]	15	216 × 288	11	28
50Salads [59]	5	216 × 288	19	50

when working with video data. In the following, we aim

to clarify how we computed scores and why we chose the respective strategies.

F.1. Phase Recognition

F.1.1 Accuracy:

- *Computation:* We follow TeCNO [12] and compute the mean video-wise accuracy, i.e. we compute an accuracy score per video and average.
- *Justification:* We chose accuracy over the F1 or Jaccard scores as our main evaluation metric since, in our experience, it is less noisy in the specific task of phase recognition. Since phase transitions are often not well defined, short phases contain a greater proportion of noisy ground-truth. In phase-wise metrics like F1 or Jaccard, these regions have a higher impact on the overall score compared to accuracy since phase transitions are only a minor percentage of the overall video length. We do, however, also report F1 scores in Table 6 of the supplementary material. The same tendencies can be seen but differences are sometimes not as clear as with accuracy. E.g. the proposed end-to-end GN-model outperforms the 2-stage state of the art TeCNO in both accuracy (90.5 ± 0.9 vs. 89.4 ± 0.8) and F1 (83.9 ± 0.7 vs. 83.4 ± 1.2) but only for accuracy the margin is larger than the standard deviation.

F.1.2 F1 Score:

- *Computation:* We compute the frame-based confusion matrix over the entire test set, compute single F1 scores for each phase and average over phases.
- *Justification:* Here, we deviate from previous work which computes mean video-wise scores. We do this to avoid ambiguities and discontinuous behavior for videos where not all phases occur or are predicted. In previous work, this was done inconsistently. E.g. Trans-SVNet [22] and TMRNet [35] set all metrics for non-occurring phases as undefined (including precision and jaccard), while TeCNO [12] use the standard definition for precision (i.e. it is only undefined if a phase is not predicted). While the first essentially ignores errors (although these errors are still captured in the recall scores of other phases), the second leads to discontinuities: Not predicting a phase at all in a video does not affect the mean precision over phases, while a single falsely predicted frame sets the precision for that phase to zero and causes a large drop in the mean over phases. This potentially favors models which ignore short, difficult phases over models which partially recognize them.

By computing F1 scores over the entire test set, these edge cases typically do not appear³. However, the disadvantage is that longer videos have a higher impact on the final score. Nevertheless, less ambiguity and not having to handle edge cases outweighs these in our opinion.

F.1.3 Relaxed Metrics for SOTA Comparison:

- *Computation:* Some methods (including the current state-of-the-art methods Trans-SVNet [22] and TMRNet [35]) report relaxed versions of metrics, which were proposed in the *M2CAI 2016 Challenge* [58]. Here, errors around phase transitions are ignored due to their ambiguity. Implementation details can be found in TMRNet’s code⁴.
- *Justification:* For our main evaluation, we opt for the non-relaxed metrics, since they are more intuitive and easier to implement and reproduce. For the state-of-the-art comparison, however, we also report relaxed scores for fair comparison and observe that our hypotheses still hold under these metrics.

F.2. Instrument Anticipation

F.2.1 Weighted Mean Absolute Error (wMAE):

- *Computation:* We follow the original instrument anticipation approach [50] and report *wMAE* as our main metric. This is the mean of the frame-wise mean absolute errors inside (*inMAE*) and outside (*outMAE*) of the horizon.
- *Justification:* We believe this is currently the anticipation metric which captures performance in the most complete way. The *inMAE* and *eMAE* used in previous work [77] do not capture errors outside of the horizon. A simple *MAE* favors conservative models which rarely anticipate instruments, since the areas outside of the horizon are much longer than inside.

F.3. Standard Deviation

- *Computation:* We compute the standard deviation of the sample (denominator $n - 1$ for n samples) over 3 training runs for our main evaluation for phase recognition and anticipation. Only for state-of-the-art comparison in phase recognition, we follow previous work and report the sample standard deviation over videos.

³Only in models which never predict certain phases and are therefore not useful anyways.

⁴<https://github.com/YuemingJin/TMRNet/blob/main/code/eval/result/matlab-eval/>

- *Justification:* We find variation over runs more informative than over videos since it captures how consistent or replicatable its performance is. On the other hand, variation over videos is difficult to interpret since videos vary highly in difficulty. I.e. even if model A consistently outperforms model B on each video, the variation over videos might still be high simply because the difficulty and thus the performance per video varies. Thus we opt to use variation over runs for our main analysis like in TeCNO [12], but have to resort to variation over videos in the SOTA comparison for phase recognition in order to stay consistent with prior work.